Jang, Minjeong; Fliri, Lukas; Trogen, Mikaela; Choi, Dongcheon; Han, Jeong Heum; Kim, Jungwon; Kim, Sung Kon; Lee, Sungho; Kim, Sung Soo; Hummel, Michael

Accelerated thermostabilization through electron-beam irradiation for the preparation of cellulose-derived carbon fibers

Published in:
Carbon

DOI:
10.1016/j.carbon.2023.118759

Published: 31/01/2024

Document Version
Publisher's PDF, also known as Version of record

Carbon 218 (2024) 118759

Contents lists available at ScienceDirect

Carbon

journal homepage: www.elsevier.com/locate/carbon

Accelerated thermostabilization through electron-beam irradiation for the preparation of cellulose-derived carbon fibers

Minjeong Jang [a,b,1], Lukas Fliri [c,1], Mikaela Trogen [c], Dongcheon Choi [a,b], Jeong-Heum Han [a], Jungwon Kim [a], Sung-Kon Kim [b], Sungho Lee [a,d], Sung-Soo Kim [a,*], Michael Hummel [c,**]

[a] Carbon Composite Materials Research Center, Korea Institute of Science and Technology, 92 Chudong-ro, Bongdong-eup, Wanju-gun, Jeollabuk-do, 55324, Republic of Korea
[b] School of Chemical Engineering, Jeonbuk National University, 567 Baekje-daero, Jeonju-si, Jeollabuk-do, 54896, Republic of Korea
[c] Department of Bioproducts and Biosystems, School of Chemical Engineering, Aalto University, 00076, Aalto, Finland
[d] Department of Quantum System Engineering, Jeonbuk National University, 567 Baekje-ro, Deokjin-gu, Jeonju, Jeonbuk, 54896, Republic of Korea

ARTICLE INFO

Keywords:
Electron-beam irradiation
Cellulose
Lignin
Accelerated thermostabilization
Carbon fiber

ABSTRACT

The potential of biobased materials like regenerated celluloses as precursors for carbon fibers (CFs) is long known. However, owing to an intrinsic two pathway pyrolysis mechanism of cellulose its carbonization is accompanied with side reactions under generation of volatiles. In practice, this leads to a reduced char yield, results in inferior mechanical properties of the CFs, and requires time-consuming thermostabilization procedures or wet-chemical pretreatments during production. Thus, their market share currently remains low. In ambitions to circumvent these issues, the potential of electron beam irradiation (EBI) as a dry chemical pretreatment for cellulosic CFs was investigated in this study. The conducted chemical analyses showed that high radiation dosages (2 MGy) lead to a strong depolymerization of the cellulose chains down to oligomers, while the fibrous macrostructure was preserved. Minor oxidation reactions were also evident. Thorough thermostabilization experiments under air in the temperature range from 100 °C to 250 °C revealed that reactions caused by EBI treatment alone were insufficient to increase the char yield. Only when the EBI treated precursor fibers are subjected to heating between 200 and 250 °C the char yield increased significantly to 34.4 % compared to 12.1 % for the untreated fiber. Furthermore, the EBI treatment strongly accelerated the reactions during thermostabilization allowing to collect CFs at heating rates of 2 °C/min compared to 0.5 °C/min needed for pristine fibers. Additionally, cellulose-lignin composite fibers were subjected to EBI treatment, proving that this strategy can also be applied to these emerging biobased CF precursors.

1. Introduction

Carbon fibers (CFs) have drawn great attention as a next-generation high-performance material which can be applied in aerospace, sporting goods, wind energy, automobile, electronics, and civil engineering industries due to their superior specific strength [1,2]. For example, CFs normally have higher ultimate strength but 4–5 times lower density (1.7–2.0 g cm^{-3}) than steel (7.7–8.0 g cm^{-3}), a standard material for construction and industrial applications [3]. As the demand of lightweight but strong composite materials has substantially increased to produce more fuel-efficient vehicles (*i.e.* Boeing's 787 Dreamliner) [4], the market of CFs for composite materials is projected to grow dramatically over the next decades [5]. To fabricate CFs with high mechanical properties, polyacrylonitrile (PAN)-based polymeric compounds have emerged as representative starting materials for the preparation of carbonizable precursor fibers. They account for more than 95 % of raw materials for worldwide CF production, owing to the high attainable tensile strength and modulus [5–7]. However, more than half of the total cost of manufacturing PAN-based CF is represented by the precursor fibers [3]. Therefore, if a low-cost precursor fiber can substitute for conventional PAN, cost issues associated with CF manufacturing can be effectively addressed.

* Corresponding author.
** Corresponding author.
E-mail addresses: sskim@kist.re.kr (S.-S. Kim), michael.hummel@aalto.fi (M. Hummel).
[1] These authors contributed equally to this work.

https://doi.org/10.1016/j.carbon.2023.118759
Received 18 September 2023; Received in revised form 8 December 2023; Accepted 21 December 2023
Available online 28 December 2023

Well-known cost-effective precursors are pitch compounds derived from coal or petroleum residues. However, an inherent unfavorable molecular weight distribution of pitch precursors and the presence of impurities (*i.e.* coke, inorganics, ash, etc.) are attributable to their poor melt spinnability [8]. Although a range of pretreatments such as air-blowing [9], distillation [10], supercritical extraction [11], and centrifugation [12] have been studied to obtain an effectively spinnable pitch precursor, these additional process steps cause an increase in the

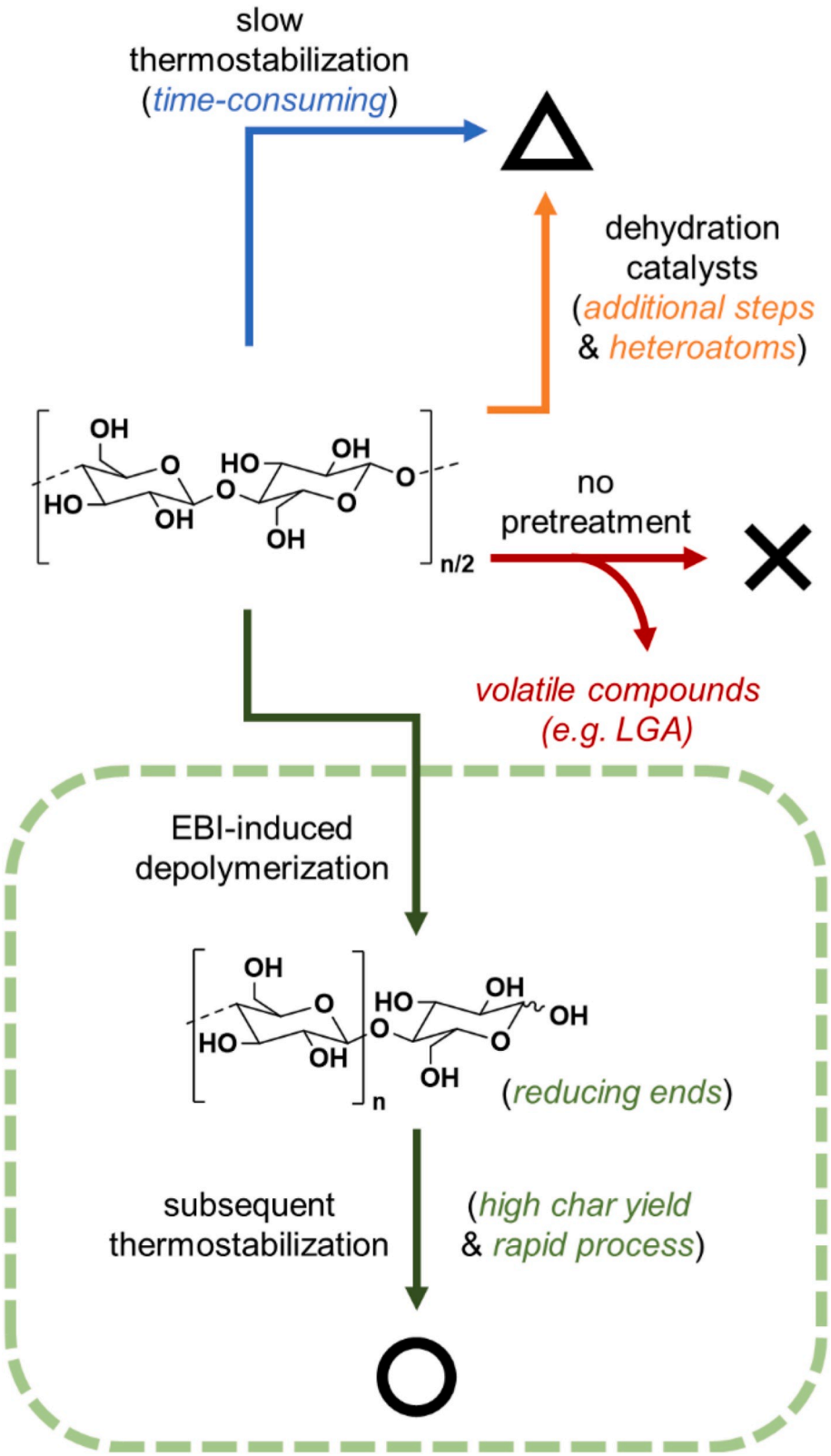

Fig. 1. Schematic illustration of different pretreatment strategies for cellulose fibers. The green-dashed box indicates the process employed and investigated in this study. (A colour version of this figure can be viewed online.)

cost of preparing pitch-based CFs [13,14]. This is regarded as one of the reasons why the use of pitch compounds as a CF precursor has been limited. Furthermore, given the drastic and noticeable issues associated with climate change, not only economic factors but also the ecological footprint of potential alternatives need to be considered. Consequently, a growing number of studies has focused on reducing emission of greenhouse gases and consumption of fossil fuels by utilizing renewable biosources as sustainable alternatives to petroleum-derived feedstocks [15,16].

Of the diverse bio-based carbon precursors, cellulose, as the most abundant biopolymer in the biosphere, is a potential candidate as a low-cost and renewable substitute. In fact, the earliest utilization of cellulose as a carbon precursor dates back to the nineteenth century by preparing carbon filaments in light bulbs from carbonized cellulose fibers [17,18]. Currently, carbon fibers derived from cellulose filament precursors are only used for niche applications, such as heat insulation (*e.g.*, Kelheim Fibres GmbH, M-Carbo fibres & composites) and only some manufacturers (*e.g.,* Stora Enso and Cordenka) produce cellulose precursor fibers for CF-reinforced composites. However, as stated above, the precursor that currently dominates the CF market is PAN, and the market share of cellulose-based CFs is negligible [19]. The average tensile strength of commercially available cellulose-derived CFs is 0.5–1.5 GPa, and their Young's modulus can be increased beyond 100 GPa when thermally treated at temperatures higher than 2000 °C [5,20,21]. Nevertheless, these mechanical properties are generally inferior to PAN-based CFs, failing to meet high-performance requirements of industries.

Another notable obstacle for the use of cellulose as a carbon precursor is the high total mass loss of cellulose precursor fibers during carbonization (~90 wt%), which likewise also contributes to the inferior mechanical properties [6]. It is well known that cellulose undergoes two competing pyrolysis pathways either resulting in a volatile tar fraction with levoglucosan (LGA) as its major constituent, or in the formation of char as a solid residue in combination with gaseous H_2O, CO_2 and CO [22–26]. While the exact mechanistic occurrences are still not agreed on, the temperatures below 300 °C were identified as most important for the final product distribution [27,28]. When applying non-optimized carbonization conditions, the majority of the cellulose repeating units is effectively lost through expulsion of LGA and other volatiles from the solid fractions, contributing to a remarkable mass reduction of the resulting carbonaceous residue (see red path in Fig. 1) [29–31]. For this reason, practical char yield of cellulose is much lower than its theoretical maximum carbon value of 44.4 wt%. Thus, it is of prime importance to increase the char yield for improving the production efficiency of cellulose-derived CFs. Given the longstanding research interest into the topic, several strategies to increase the char yield have been proposed. For example, thermostabilization through slow heating rates or longer isothermal treatments around 250 °C have shown a considerable effect on the char yield (see blue path in Fig. 1) [27,28]. However, in practice they present no viable option, as they drastically reduce the material throughput [32,33]. To shorten the period of the thermostabilization process, cellulose fibers were treated with acids [34] or dehydration catalysts [35,36] prior to the thermal treatment (see orange path in Fig. 1). These reagents are postulated to catalyze the dehydration of cellulose repeating units [6,37,38], resulting in an increased char yield (up to 25–30 wt%) by accelerating the thermostabilization and mitigating the generation of volatiles following the tar forming reaction pathway. However, the application of dehydration catalysts again leads to additional process steps, *e.g.*, by the needed immersion of the cellulose precursor fibers in a water bath or the subsequent removal of potentially hazardous compounds from the expulsed volatiles (*e.g.*, ammonia from the used phosphate or sulfate salts or the added acids themselves) [39–41]. Furthermore, it can result in the incorporation of considerable quantities of heteroatoms like sulfur or phosphorus in the solid fractions after thermostabilization, which might influence the high temperature treatments up to 2000 °C, needed to enhance the mechanical properties [42,43].

Dry chemical processes without using solvents or additional chemicals were proposed several times for modulating the chemical structure of PAN or pitch-based CF precursors. For example, the treatment by plasma [44–46], gas molecules ionized in the presence of an external electric field or heat, effectively tunes the hydrophilicity of the fiber surface by activation or functionalization [47]. This plasma treatment quantitatively controls the chemical and topographical properties by various parameters of the plasma process [48]. Similarly, treatment with electron-beam irradiation (EBI) was investigated. EBI has been particularly known for its high energy efficiency, short throughput time, fair uniformity, and environmental friendliness [49]. Chemical bonds within PAN precursor fibers can be dissociated by the irradiation of electron beam, under the generation of free radicals and subsequent coupling with atmospheric oxygen. These continuous reactions lead to the modification of polymeric structures by cleavage, crosslinking, and grafting even before the thermal oxidation process [50]. Such chemical transformations effectively accelerate the thermostabilization process of PAN by the structural modification induced by radical-assisted pre-oxidation [51–53].

Given the known intrinsic benefits of dry chemical pretreatments and accumulating know-how in operating EBI treatments for other CF precursors, we were tempted to investigate the possibilities of EBI in the fabrication of CFs from cellulosic precursors (see green path in Fig. 1). This may allow for a more extensive application of biobased CFs by reducing the total expense of CF preparation. Nonetheless, owing to the stark differences in the structures of cellulose compared to PAN or pitch, it is obvious that application of EBI also results in different chemical reactions during the treatment and the subsequent thermostabilization, necessitating careful analysis and optimization of the process. Most studies focusing on EBI treatment of cellulose agree that it predominantly results in partial depolymerization of the chains in combination with partial oxidation of the anhydroglucose (AGU) repeating units – with varying degrees depending on the applied dosage [54]. However, Henniges *et al.* noted that the extend of oxidation is often overestimated as the applied analytical techniques are also sensitive towards the carbonyl functionalities of the reducing end groups (REGs) liberated during the partial depolymerization [54]. Furthermore, they also argue, "that several aspects of the interaction between cellulose and electron beam irradiation are still far from being sufficiently understood". To the best of our knowledge only one study addressed cellulose EBI treatment in the explicit context of CF production [55]. A modest increase in the char yields was observed, which was ascribed to crosslinking over ester bridges formed from EBI-induced oxidized moieties. However, in this report the effects of subsequent thermostabilization were not further examined.

In the study at hand, fibers spun from cellulose and cellulose-lignin mixtures were treated with electron beam, followed by thermostabilization (up to rapid heating rates of 2 °C/min) and carbonization to prepare cellulose-derived CFs. To confirm the effect of EBI pretreatment and obtain a better understanding of its consequences, the chemical transformations in the cellulosic precursors were analyzed with a variety of analytical techniques, including electron spin resonance (ESR), Fourier transform infrared (FTIR) and a solution state nuclear magnetic resonance (NMR) spectroscopy protocol devised for cellulosic materials [56]. Furthermore, changes in the molecular structure and thermal behavior in the precursor macromolecule upon the subsequent thermal treatment were studied. Compared to the duration of conventional thermostabilization with no pretreatment, we verified that thermostabilization after EBI required much less time and resulted in significantly increased char yields. This confirms that the pretreatment of the cellulose fiber by EBI can effectively decrease the time and energy consumption for manufacturing cellulose-derived CFs.

2. Experimental section

2.1. Materials

Pre-hydrolyzed kraft (PHK) birch pulp ([η] = 494 ml/g) was received from Stora Enso Enocell mill in Finland and Organosolv (ethanol/H_2SO_4) beech lignin (BL) from the Lignocellulosic Biorefinery Pilot Plant, Fraunhofer CBP in Leuna, Germany. The pulp was received as sheets and ground using a Wiley mill to a fine powder. The lignin was used as received. For the preparation of ionic liquid, 1,5-diazabicyclo [4.3.0]non-5-ene (DBN) (Fluorochem, UK) and acetic acid (glacial, 100 %, Merck, Germany) were used. DBN and acetic acid were used as received. PAN-based carbon fiber (T700S) was purchased from Toray, Inc., Japan.

2.2. Precursor spinning

Precursor cellulose and cellulose-lignin filaments were prepared using the Ioncell® process as described earlier [57]. In short, DBN was mixed with acetic acid in a glass reactor with cooling (25 °C) and after the slow addition of acid the solution was mixed for an hour at 75 °C. Pulp and lignin were dissolved in the ionic liquid using a vertical kneader (80 °C, 90 min, 7 ± 3 mbar, mixing 30 rpm). The dissolved cellulose or cellulose-lignin mixtures were filtered (pore size 5 μm) and then dry-jet wet spun using a piston-spinning unit (Fourné Polymertechnik, Germany), with an air gap of 1 cm. A spinneret with 400 holes, capillary diameter 100 μm and L/D 0.02 was used. The spinning solution was extruded at 5.5 mL/min and at 71 ± 5 °C into an aqueous coagulation bath, and the take-up velocity was adjusted to a draw ratio of 6. After spinning, the fibres were washed with tap water using a custom-made washing line (washing: 10 ± 0.25 min retention time at 68 ± 3 °C) and dried at 80 °C.

2.3. E-beam irradiation

Prior to the thermostabilization process, EBI of the cellulose fiber was carried out at room temperature using an electron beam linear accelerator (2.0 MeV) at the Advanced Radiation Technology Institute, Korea Atomic Energy Research Institute (Jeongeup, Republic of Korea). In this work, cellulose and cellulose-lignin composite fibers are denoted as "C [the irradiation dose in MGy] E," and "CL [the irradiation dose in MGy] E," respectively (see Table S1).

2.4. Thermostabilization and carbonization

Thermal stabilization was performed by fixing the pristine fibers to a thermal stretching machine. The irradiated samples were subsequently placed in a convection oven at 50 °C. Then the temperature was elevated to $T_{f,t}$ (the final temperature of thermostabilization) at the elevation rate of 0.2, 0.5, 1, and 2 °C/min in air without intervals of holding temperature. The sample name of thermostabilized fibers was described as "C (L) [the irradiation dose in MGy] E [$T_{f,t}$] S"

The stabilized fibers ($T_{f,t}$ = 250 °C) were taken out from the thermal drawing machine and fixed to the graphite sheet with carbon tape to conduct carbonization. The stabilized fibers were carbonized in a furnace, and the temperature was increased from 25 °C to 1000 °C at the heating rate of 5 °C/min in Ar atmosphere. The sample name of carbonized fibers was described as "C(L) [the irradiation dose in MGy] ESC_ [the elevation rate during thermostabilization in °C/min]" (see Table S1).

2.5. Characterization

Electron spin resonance (ESR) spectroscopy was utilized to identify the generation of radicals in the fibers using a JES-FA100 spectrometer (JEOL, Japan). A Nicolet iN10 infrared microscope (Thermo Scientific, USA) was used to collect FT-IR spectra from the stabilized fibers with a slide-on attenuated total reflection (ATR) accessory (MicroTip Ge crystal) and an MCT (mercury−cadmium−telluride) detector cooled by liquid N_2. Nuclear magnetic resonance (NMR) spectra were recorded with a Bruker Avance III 400 NMR spectrometer. For the dissolution of the EBI treated and thermostabilized cellulosic precursor fibers a [P_{4444}][OAc]:DMSO-d_6 (1:4 wt%) electrolyte was used, closely following a recently reported protocol [56]. All samples were investigated using quantitative ^{1}H, diffusion edited ^{1}H and ^{1}H–^{13}C HSQC experiments. Peak assignments were based on previous reports utilizing the same solvent system [56,58–60]. All obtained spectra were summarized in the supporting information to an NMR spectral catalogue (Fig. S6 - **S27**). Thermogravimetric analysis (TGA) to investigate continuous changes in the weight of cellulose and composite fibers during the stabilization and carbonization process, respectively, was performed by use of a TA Instrument SDT 650 (USA). The differential scanning calorimetry (DSC) measurements of the fibers were carried out on a DSC 4000 (PerkinElmer, USA) in air. Mass fractions of carbon, hydrogen, nitrogen, and sulfur in fiber samples were determined by elemental analysis (EA) by use of a Thermo Scientific Flash 2000 (USA). Oxygen values were calculated by subtracting the total of the other four elements (C, H, N, and S) from 100 %. X-ray diffraction analysis (XRD, SmartLab, Rigaku, Japan) was conducted for the crystalline structure of fiber samples under a scan speed of 4°/min in the range of 10°–60° using Cu K_α radiation (λ = 1.54 Å) of 45 kV and an emission current of 200 mA. Fiber morphology was observed through optical microscopy (OM, Nikon Eclipse Ni–U, Japan) and scanning electron microscopy (SEM, NOVA NanoSEM 450, FEI, USA). The surface of the fiber samples was coated with a thin Pt layer by an SPT-20 Ion Sputter Coater (COXEM Co., Ltd., Korea) for SEM. Raman spectra were obtained using a Raman spectrometer (Renishaw, U.K.) equipped with an AR-ion laser (λ = 514 nm). The laser beam was focused by a 100 × objective lens, resulting in a spot size of approximately 1 μm in diameter. The mechanical properties of the carbonized fibers were evaluated using an individual fiber test system (FAVIMAT+, Textechno, Germany). The gauge length and testing speed were 25 mm and 5 mm/min, respectively. Twenty filaments were measured for each sample. Densities of the fibers were measured by using a density gradient column filled with mixed liquids, which were made of benzene and 1,1,2,2-tetrabromoethane. Glass beads with accurately known densities floated in the column, and each fiber of at least three species was inserted into the column and left for 12 h. Then the density of the fiber was calculated based on its relative position to the beads in the column and the densities of the glass beads. The thermal conductivity of a carbon fiber was measured using the DC self-heating method [61]. For measuring the thermal conductivity of a fiber, the fiber sample was heated by Joule heating using DC current through the fiber. During heat generation, the temperature rise of the sample was measured by the thermoresistance of each fiber using four-point measurement. Convection and radiation heat transfer are negligible due to high vacuum (~10^{-6} Torr), and the small temperature rise below 15 K. The heat generation by Joule heating was measured with a source meter (Keithley 6221) and a nanovoltmeter (Keithley 2182A). The geometry of the fiber was measured by OM to evaluate its length and cross-sectional area.

3. Results and discussion

3.1. Chemical transformation of cellulose fibers caused by EBI treatment

To understand the effects of the EBI treatment on the pristine cellulose precursor (**C0E**) in general and to examine differences between the samples treated with 1 MGy (**C1E**) and 2 MGy (**C2E**) respectively, different spectroscopic techniques were applied. Given the previous reports we especially screened for signs of partial depolymerization, radical induced oxidation and crosslinking by ester bridges.

The ESR spectra shown in Fig. 2a proved the generation of free

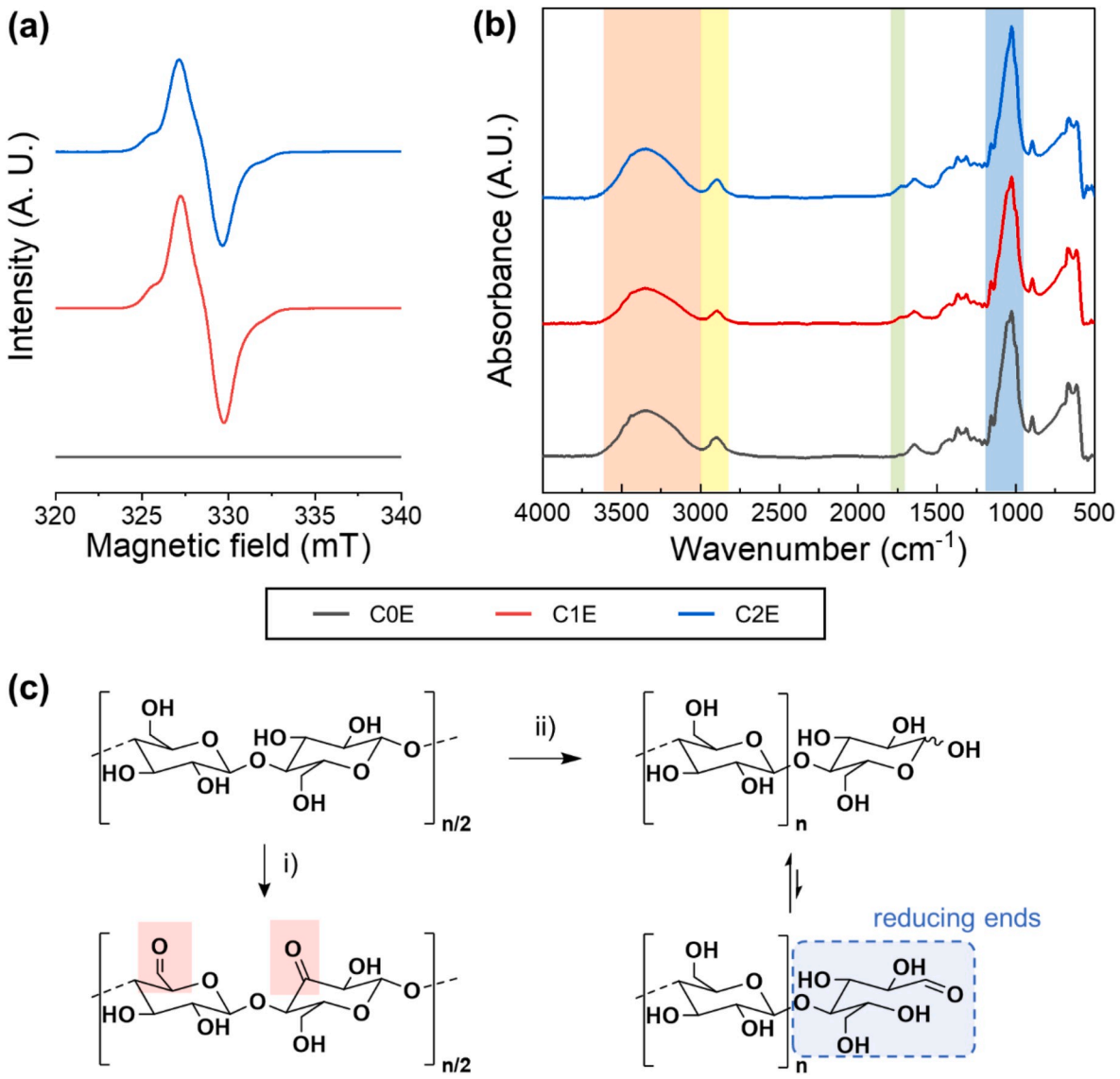

Fig. 2. (**a**) ESR spectra and (**b**) FT-IR spectra of pristine and irradiated cellulose fibers. (**c**) Reaction pathways for cellulose under EBI. Based on our chemical characterization pathway **ii** dominated in the treated cellulose fibers. (A colour version of this figure can be viewed online.)

radicals in **C1E** and **C2E,** while expectedly no signal was observed for sample **C0E**. The observed *g*-values corresponded to that of carbon-centered organic radicals. This observation confirmed that EBI forms radical species in the fiber [62–65]. Moreover, these radical species did not immediately undergo follow up or recombination reactions, but remained fairly stable in the cellulosic material as there was a considerable time gap between EBI treatment and collection of the ESR spectra (as long as 24 h).

In the FT-IR spectra absorption bands associated with stretching modes of O–H (3000–3600 cm^{-1}; orange box), C–H (2800–3000 cm^{-1}; yellow box), and C–O (900–1200 cm^{-1}; blue box) were the most dominant (Fig. 2b). There was a negligible difference between FT-IR spectra of **C0E** compared to the EBI treated samples, except for the introduction of a small band at 1720 cm^{-1}, which can be ascribed to the stretching mode of carbonyl groups.

Already during the dissolution of the samples for NMR characterization partial depolymerization reactions caused by EBI treatment were indicated, based on the markedly reduced viscosities of the resulting solutions compared to the pristine precursor [56]. This was confirmed in the NMR spectra by the appearance of peaks for reducing end groups (REGs) and non-reducing ends (NREs) especially in the ^{1}H–^{13}C HSQC spectra (see Fig. S12 and **S15;** REG resonances for C1–H-β: ^{1}H = 4.21/^{13}C = 97.6 ppm; for C1–H-α: ^{1}H = 4.91/^{13}C = 91.9 ppm; NRE resonances for C1–H: ^{1}H = 4.30/^{13}C = 102.6 ppm) [59]. Additionally, indirect evidence for the occurrence of partial oxidation reactions during EBI (reaction pathway (i) in Fig. 2c) was obtained in the ^{1}H spectra by the presence of low-molecular weight degradation products in the range of 8–10 ppm (see Figs. S10 and S13). Similar degradation phenomena in the electrolyte system leading to the formation of a formate (peak around 8.6 ppm) were observed in periodate oxidized celluloses [66] and can be ascribed to reactions of the basic acetate anion with the oxidized moieties, following a beta elimination mechanism [67]. However, in accordance with the FT-IR results oxidation occurred only to a minor extent. The spectra even for **C2E** after treatment with 2 MGy are dominated by signals of the AGUs.

Owing to peak superposition of the REG and NRE signals with the water peak and xylan contents needed to calculate the degree of polymerization (DP) from the NMR spectra [59], it was not possible to examine the extent of depolymerization caused by EBI treatment more accurately. However, additional insights in this matter were obtained from the diffusion edited ^{1}H experiments. This experiment suppresses signals of low molecular mass constituents present in the NMR samples

in the spectra and only leaves peaks of polymeric materials behind. A molecular weight cut-off is applied to effectively remove the strong peaks of the non-deuterated electrolyte, also resulting in the removal of signals of short cellulose chains below a DP_N of approximately 10–15. In the comparison of the diffusion edited ^1H spectra of **C1E** and **C2E** the only significant difference between the differently treated precursors became evident. While strong depolymerization was also evident in **C1E** there were still cellulosic peaks visible in the diffusion edited experiment, meaning that fractions with a $DP_N > 15$ were present in the sample (see Fig. S11). Instead, in **C2E** the diffusion editing removed all peaks, and no polymeric material was evidenced. Further examination of the ^1H–^{13}C HSQC spectra revealed that no complete depolymerization to either cellobiose or glucose occurred either. Their resonances in the used electrolyte were recently assigned by Koso et al. [58]. Given the superimposing degradation mechanism of the oxidized moieties in the electrolyte it is not meaningful to estimate the DP of the EBI treated fibers based on these spectra. However, as the peaks of the low molecular weight degradation products in both **C1E** and **C2E** were similar, their difference in oxidized units seems to be minor. Thus, the major difference between the samples can be found in the stronger depolymerization caused by the harsher EBI treatment. Despite this strong depolymerization, the precursor fibers maintained their structural integrity and crystallinity (see Fig. S1. In conclusion, the results of the chemical analysis reflected the outcome expected from literature [54]. The EBI treatment resulted in the dissociation of bonds in the cellulose chains following a radical mechanism, resulting in strong depolymerization owing to the cleavage of 1–4 glycosidic bonds (reaction pathway (ii) in Fig. 2c) and slight oxidation of the AGU repeating units. The generation of REGs as observed in the NMR spectra mechanistically requires a reaction with water. Given the presence of stable radicals in the ESR spectra, we cannot rule out that this reaction only occurs during dissolution in the NMR electrolyte, and radicals are still present during the subsequent thermostabilization steps. However, owing to the presence of around 2–3 wt% of water (Fig. 3) on the surface of the treated fibers and the generally low limit of detection of ESR, we surmise that the REGs are predominantly formed already in the solid state by reaction with ambient water. Instead, we did not observe any signs of direct crosslinking caused by EBI treatment, *e.g.*, through postulated ester bridges [55].

3.2. Effect of EBI on the thermostabilization of cellulose precursor fibers

3.2.1. Thermal stability of precursor fibers

Thermostabilization prior to carbonization at high temperature is known to be crucial for successful CF production with reasonable yields. Hence, it is important to understand the chemical reactions in the EBI treated cellulosic precursor fibers during the thermal treatment in air to determine optimal conditions for the thermostabilization and achieve high char yields.

For this purpose, TGA thermograms were obtained from pristine and irradiated cellulose fibers (Fig. 3), and the change in the mass of those fibers was recorded during the heating process at a rate of 2 °C/min in air to simulate thermostabilization conditions used for the subsequent preparation of CFs. All fiber samples showed a stepwise reduction in relative mass upon heating in air regardless of the irradiation dose, which can be divided into three regions (**I**, **II**, **III** in Fig. 3). A small weight loss is first observed at the region **I** (≤100 °C), attributed to the release of physically adsorbed water in cellulose. Compared to the small mass change in region **I**, the decrease within region **II** (250–350 °C) is significantly higher. A number of previous studies regarding the thermal behavior of cellulose indicated that the drastic mass reduction in this region is closely related to the thermally induced decomposition of cellulosic macromolecules following the generation and expulsion of volatiles, with LGA as major product [6]. Finally, carbonaceous residues are completely degraded through reactions with oxygen in the region **III** (400–500 °C). As a severe mass loss during the thermostabilization may have an adverse effect on the structural integrity of fibers after thermal treatment and ultimately the mechanical properties of the resulting CFs, 250 °C was selected as the final temperature of the thermostabilization step in this study. The relative mass loss of the irradiated samples was less than 10 wt%.

Despite a similar overall thermal behavior shown by TGA thermograms, there was a notable difference between pristine and irradiated cellulose fibers in region **II**; the irradiated samples clearly exhibit an earlier onset of thermal decomposition compared to the pristine cellulose. For example, temperatures of 10 % mass loss ($T10\%s$) of **C1E** (278.0 °C) and **C2E** (263.2 °C) were lower than that of **C0E** (291.6 °C) (see the dashed horizontal line in the magnified plot of Fig. 3), implying that the EBI-induced depolymerization enabled thermal reactions at relatively low temperatures (≤250 °C). Hence, it is expected that the subsequent thermostabilization would induce effective chemical transformations only in the irradiated fibers.

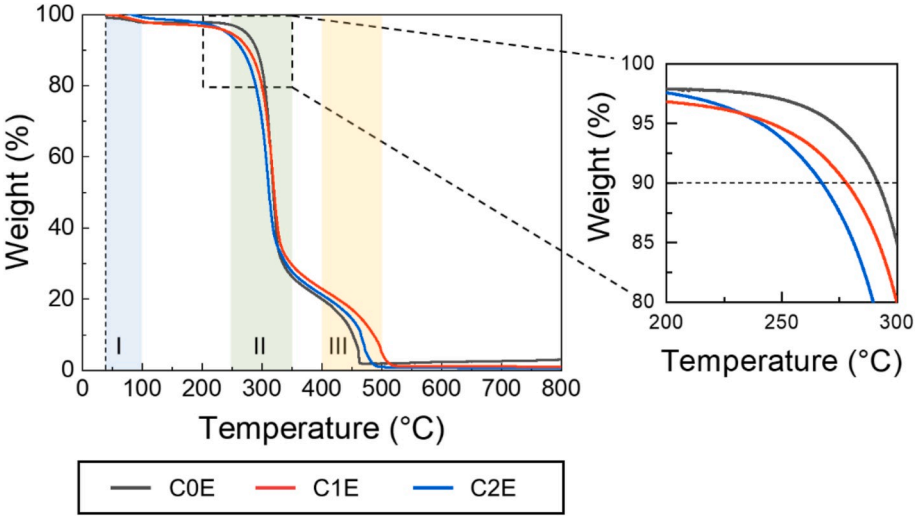

Fig. 3. TGA thermograms (air) of pristine and irradiated cellulose fibers. Heating rate for the TGA analyses was 2 °C/min. The dashed vertical line indicates 40 °C, the initial temperature of the TGA analyses. (A colour version of this figure can be viewed online.)

3.2.2. Optimization of the thermostabilization

After evaluating the general stability limits of the irradiated fibers during heating in air, we set out to determine the temperature ranges with the most profound influence on the char yields. The effects of the oxidative pretreatment at different final thermostabilization temperatures ($T_{f,t}$) between 100 °C and 250 °C were examined. The respective samples are summarized in Table S1.

DSC thermograms of the pristine and irradiated fibers with and without subsequent thermostabilization at different $T_{f,t}$ (Fig. 4) were measured. In all thermograms, an endothermic reaction was observed at temperatures lower than 100 °C, which is related to the evaporation of water which re-adsorbed on the thermostabilized fibers during storage. Non-irradiated samples showed no significant additional thermal reactions in the temperature range up to 300 °C (Fig. 4a), which was expected given the higher thermal stability observed in Fig. 3. In contrast, the irradiated fibers with a $T_{f,t}$ up to 200 °C experienced another endothermic reaction as the temperature reached 300 °C (blue dashed box). As the volatilization of LGA during cellulose pyrolysis is endothermic [68], this reaction is likely linked to an earlier thermal decomposition of the irradiated samples (region **II** of Fig. 3) following the tar forming pathway. In other words, the generation of REGs through EBI can promote the formation of LGA over dehydration and unzipping in those not sufficiently thermostabilized samples. Conversely, **C1E250S** and **C2E250S** (thermograms in purple color in Figs. 4b and 3c, respectively) exhibited an exothermic reaction as the temperature reached 300 °C (red dashed box). This different thermal behavior was observed only when the thermostabilization temperature $T_{f,t}$ was 250 °C, suggesting that heating at 2 °C/min in the temperature range of 200–250 °C and under air leads to a critical chemical change in the EBI-treated cellulose matrix. It is worthwhile to note here again that **C1E250S** and **C2E250S** went through a reduction in their relative mass when the process temperature passed the temperature range of 200–250 °C, as illustrated in the TGA thermograms of **C1E** and **C2E** (Fig. 3), which is closely related to the change in the chemical structure of cellulosic fragments decomposed by EBI.

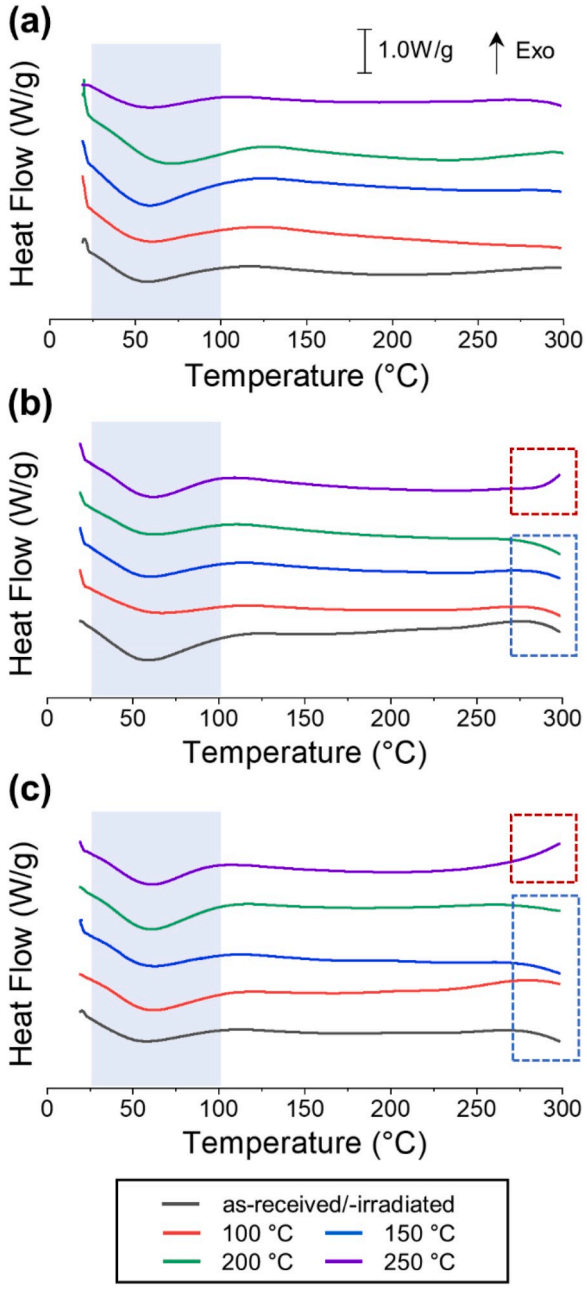

Fig. 4. DSC thermograms (air) of (**a**) **C0E**, (**b**) **C1E**, and (**c**) **C2E** thermostabilized with different $T_{f,t}$. (as indicated in the legend). Heating rate for the DSC analyses was 2 °C/min. (A colour version of this figure can be viewed online.)

The thermal reactions in the temperature range of 200–250 °C had a significant effect on the final char yield after carbonization. Fig. 5 shows the TGA thermograms of non-thermostabilized fibers (**C0E**, **C1E**, and **C2E**; dashed plots) and thermostabilized fibers with $T_{f,t}$ = 250 °C (**C0E250S**, **C1E250S**, and **C2E250S**; solid plots). Char yields of fibers at 1000 °C are listed in Table S2. Regardless of EBI, there was no significant difference in the char yield at 1000 °C among non-thermostabilized fibers (12.1 % for **C0E**, 12.7 % for **C1E**, and 11.8 % for **C2E**). Thermally induced chemical reactions during thermostabilization were indispensable for increasing the char yield. **C0E250S** showed a small increase of 2–3% in the char yield (14.7 %) at 1000 °C, implying that non-irradiated cellulose was affected by the thermostabilization, but not completely transformed into a thermally stable structure. The chosen rapid temperature ramp of 2 °C/min did not provide a sufficiently long period for the chemical transformation of the cellulosic precursors. Thus, predominantly volatile compounds are released following the competing pathway during carbonization, ultimately resulting in the low char yield. However, **C1E250S** and **C2E250S**, the irradiated and thermostabilized fibers with a $T_{f,t}$ of 250 °C gave rise to a higher carbonaceous residue of 24.6 and 34.4 %, respectively after carbonization at 1000 °C. This suggests that the combination of EBI and subsequent thermostabilization is of prime importance for enhancing the char yield. However, TGA thermograms of the irradiated fibers with different $T_{f,t}$ showed that this considerable increase in the char yield was only observed when $T_{f,t}$ was 250 °C (Fig. 5b and c). In other words, thermal reactions within the irradiated fibers at the temperature range of 200–250 °C must be attributable to this outcome. Notably, the earlier onset of endothermic reactions observed in the DSC experiments for non- and insufficiently thermostabilized precursors (up to $T_{f,t}$ of 200 °C) compared to the pristine cellulose indicates that the reaction pathway favoring the formation of volatiles is promoted in the EBI treated fibers. Mechanistically the generation of LGA as first and major generated volatile compound can only occur on the REG. As the strong fragmentation caused by EBI treatment drastically increased the proportion of REGs, it seems plausible that also the formation of LGA is accelerated, which is reflected in the low attainable char yields. Only during heating at 200–250 °C reactions take place which effectively suppress the generation of volatiles.

3.2.3. Chemical changes introduced by the thermostabilization

To get further insights into the chemical transformations occurring during the performed thermostabilization regimes, photographs and FT-IR (Fig. 6) spectra of the thermostabilized fibers obtained from **C0E** and **C2E** were recorded. Furthermore, the samples from **C2E** were subjected to solution state NMR analysis. Similar to our previous study on

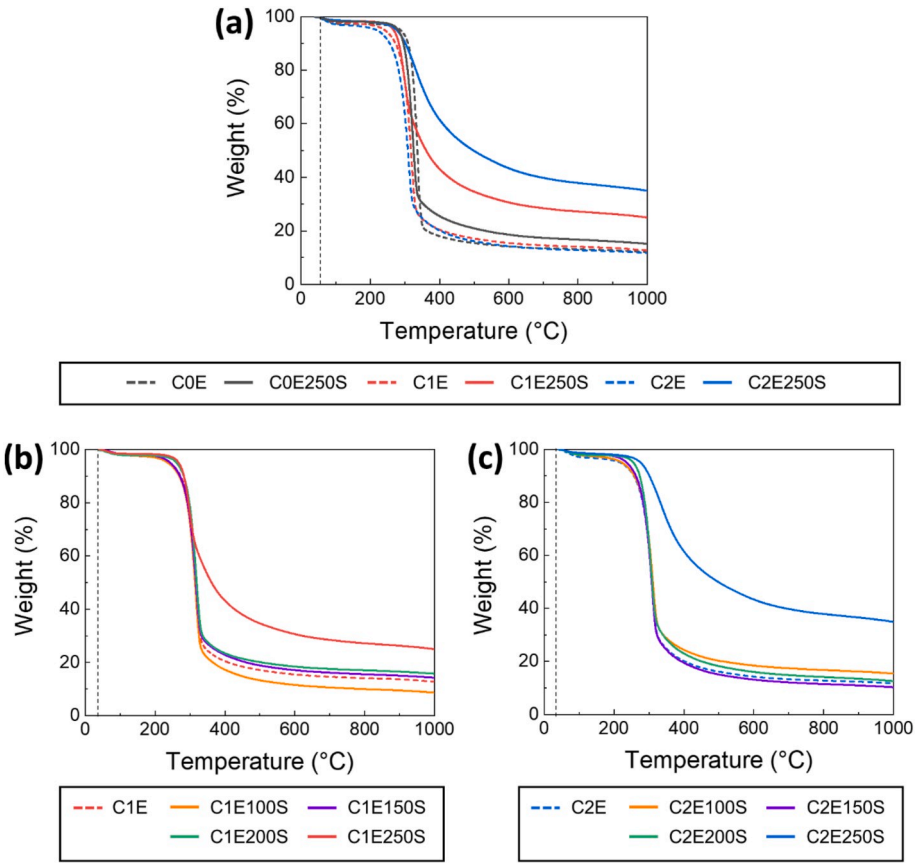

Fig. 5. TGA thermograms (Ar) of (**a**) pristine and irradiated cellulose fibers, and those after thermostabilization ($T_{f,t}$ = 250 °C), (**b**) thermostabilized **C1E**, and (**c**) **C2E** fibers with different $T_{f,t}$. Heating rate for the TGA analyses was 5 °C/min. The dashed vertical lines indicate 40 °C, the initial temperature of the TGA analyses. (A colour version of this figure can be viewed online.)

isothermal temperature treatments under inert conditions [60], there was no significant change among non-irradiated cellulose fibers until $T_{f,t}$ reached 200 °C. Thermal treatments in air at temperatures higher than 200 °C changed the color of fibers from white to brown, while absorption bands associated with stretching modes of O–H (3000–3600 cm^{-1}; orange box), C–H (2800–3000 cm^{-1}; yellow box), and C–O (900-1200 cm^{-1}; blue box) were weakened (Fig. 6a). Bands related to C═O (1700–1750 cm^{-1}; green box) and C═C (1600–1700 cm^{-1}; gray box) were detected in the spectrum of **C0E250S**, however, only in very minor intensities. Consequently, the thermostabilization of **C0E** did not significantly alter the bulk chemical composition of the fibers but was predominantly restricted to the formation of chromophores and presumably supramolecular changes [61]. These observations are in line with the results from thermal analysis shown in the previous section. In contrast, the color of **C2E250S** was almost black in spite of the same $T_{f,t}$, and the intensity of absorption bands associated with C═O and C═C groups was considerably stronger in the FT-IR spectrum (Fig. 6b). Based on the IR spectrum, the bulk material in **C2E250S** can no longer be characterized as a simple cellulosic macromolecule. Instead, the thermostabilization in the range of 200–250 °C resulted in significant chemical changes in the precursor fibers, considering the presence of carbonyl and alkene moieties, likely connected with dehydration reactions. The occurrence of dehydration reactions in **C2E250S** were further corroborated by the results of elemental analysis, where the proportion of carbon markedly increased, while the oxygen and hydrogen contents decreased (Fig. S3).

Notably, the color and spectral change in **C2E** upon rising temperature took place earlier than those in **C0E** (Fig. 6b). For example, the color and FT-IR spectrum of **C2E200S** were similar to those of **C0E250S**. In accordance with the TGA results (Fig. 3) this suggests that the EBI treatment accelerates thermal reactions in the investigated temperature ranges and shifts the onset of the reactions to lower temperatures.

Additionally, the EBI treated precursor fibers thermostabilized at different $T_{f,t}$ were examined by solution state NMR. Recently, the same approach was used in a similar study focusing on isothermal treatments in the same temperature ranges of pristine cellulose precursors under an inert atmosphere [60]. Thereby, the formation of LGA end-capped cellulose structures was identified as the first and major occurring transformation. These reactive structures were presumed to be connected with the subsequently observed thermal crosslinking reactions. Moreover, a completely insoluble phase was encountered, which showed high similarities to a previously described "thermostable condensed phase" [69,70].

In the EBI-treated fibers practically the same reactions were evident in the NMR spectra as in the previously conducted study, however, they were more pronounced and shifted to lower temperatures. While **C2E100S** did not show any additional modifications compared to **C2E** in the sample thermostabilized at 150 °C already first signs of LGA end-capped moieties were visible in the ^{1}H–^{13}C HSQC spectra, while they became dominant in **C2E200S** (see Fig. S24; LGA C1–H at ^{1}H = 5.06/^{13}C = 103.3 ppm) [60]. This reflects the earlier onset of thermal reactions compared to the pristine fibers, where the same moieties could only be clearly observed after longer isothermal treatments at higher temperatures (225–250 °C) [60]. It seems plausible that the generation of LGA moieties from the REGs introduced through EBI following dehydration is energetically preferred over the chain scission following transglycolization required in the pristine cellulose fibers. In **C2E200S** the LGA peaks become more intensive, and another peak previously connected with crosslinked polysaccharidic structures emerged (see Fig. S24; CH or CH_3 at ^{1}H = 4.26/^{13}C = 77.2 ppm) [60]. Slight

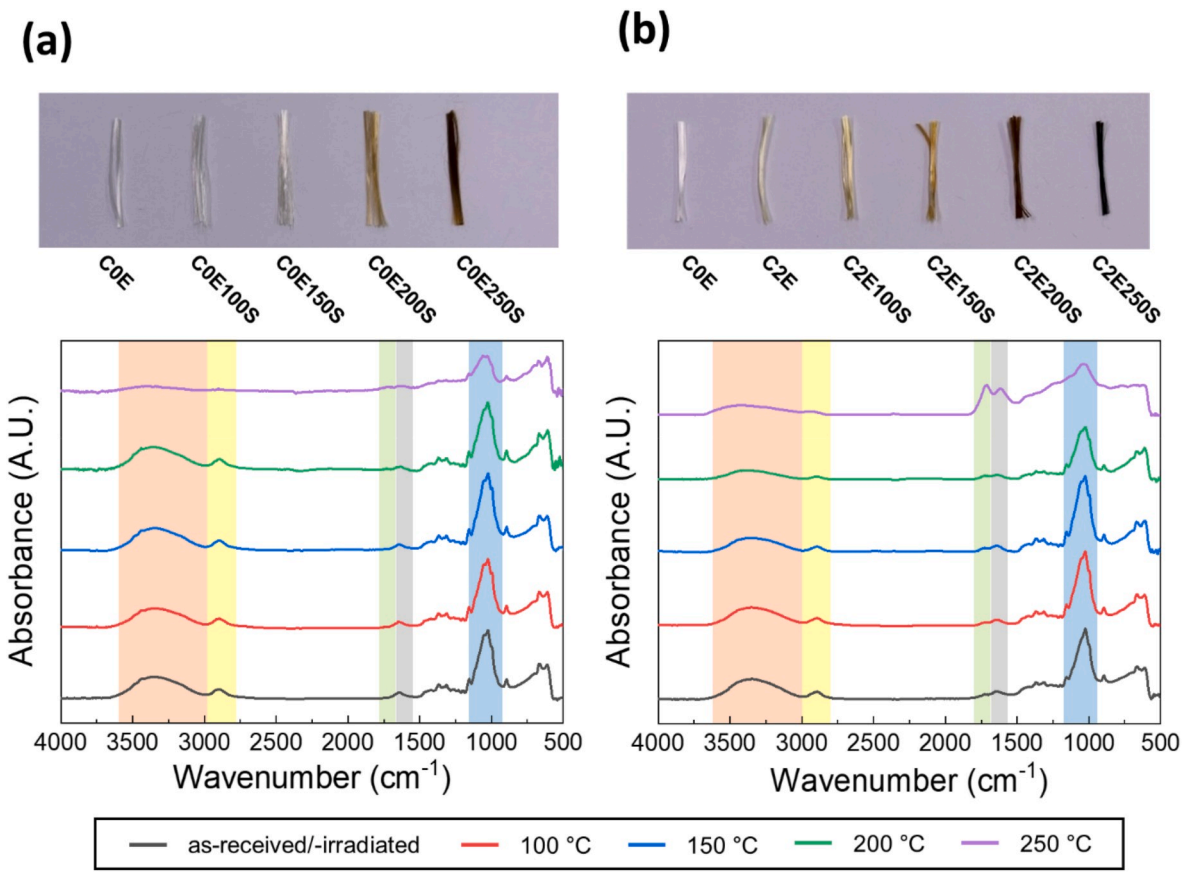

Fig. 6. Photographs and FT-IR spectra of (**a**) **C0E** and (**b**) **C2E** with different $T_{f,t}$. (A colour version of this figure can be viewed online.)

crosslinking is also supported by the diffusion edited ^{1}H spectra, where the thermostabilized fibers (**C2E150S** and **C2E200S**) exhibited longer polymer fractions with a molecular weight over the cut-off area (approximately DP_N of 10–15), as opposed to the starting material and **C2E100S** which did not. Severe oxidation reactions were not evident based on the peaks of the low molecular weight degradation products, despite conducting the thermostabilization under air.

A completely different behavior was encountered in sample **C2E250S**, which proved to be almost completely insoluble while keeping its fibrous structure. Only very minor peaks of saccharidic extracts were visible in the ^{1}H–^{13}C HSQC spectra. Also, no crosslinked polysaccharide fractions were evidenced in the diffusion edited ^{1}H experiments. In line with the FT-IR spectra and the results of thermal analysis this further suggests that marked chemical changes occurred in the temperature range from 200 to 250 °C. The insolubility of **C2E250S** in the applied electrolyte proves that the sample cannot be characterized as a linear polysaccharide. Similar observations were reported by Pastorova *et al.*, where a so called "thermostable condensed phase" was formed after heat pretreatment of pristine cellulose at 250 °C, which even resisted hydrolysis in concentrated hydrochloric acid. They emphasized that a "new polymer" is formed which predominantly consists of furanoid skeletons, hydroxyaromatic skeletons, unsaturated hydrocarbon chains, carbonyl and carboxylate functionalities [69,70]. The transformation of crystalline cellulose moieties into a new condensed phase was also implied by the X-ray diffractograms (Fig. S1), where the diffraction bands corresponding to the crystalline structure of cellulose essentially vanished after thermostabilization. Moreover, the absence of characteristic D- and G-bands in the Raman spectra (Fig. S5) suggested that no significant formation of condensed benzene rings occurred in this intermediate phase.

Based on the chemical analysis we can summarize the reactions in thermostabilized EBI treated cellulose fibers as follows (Fig. 7). The irradiation initially leads to strong fragmentation in the polysaccharide backbone through cleavage of the 1–4 glycosidic bond over formation of radicals, which result in the generation of REGs after reaction with ambient water (Fig. 7a and **Figure b**). The REGs undergo dehydration reactions to LGA end capped cellulose fragments at lower temperatures compared to the pristine precursors and subsequently result in different crosslinked polysaccharide structures (Fig. 7c). While the presence of oxidized moieties after EBI treatment was evidenced in the NMR spectra and presumably further oxidation occurs during the thermostabilization under air, we surmise that possible crosslinking over these oxidized structures only has a minor influence on the overall carbonization mechanism. Especially, as we could not see any evidence for respective hemiacetal or ester linkages in the NMR spectra of the samples thermostabilized at 200 °C, while a linkage over LGA crosslinking became visible. Nonetheless, these transformations up to 200 °C leading to crosslinked polysaccharide fractions only had an insignificant influence on the ultimate char yield according to the TGA measurements (Fig. 5).

While crosslinking was often mentioned as a factor increasing the char yield in cellulose carbonization in the literature, the exact nature of the formed bonds is still not clear. Comparing the thermal behavior and chemical analyses of **C2E200S** and **C2E250S**, which both can be characterized as "crosslinked" structures, we want to highlight that at least two different crosslinking mechanisms must be operative; the first occurs at temperatures below 200 °C over LGA end-capped cellulose fragments resulting in a network of differently linked oligosaccharide fractions (Fig. 7c). According to Kawamoto, these bonds are reversible, and the postulated structures cannot serve as an explanation for subsequent dehydration reactions operative in char formation [71]. Thus, the expulsion of volatiles, like LGA, cannot be suppressed completely. The other mechanism occurred between 200 and 250 °C and resulted in a chemically strongly altered, heavily crosslinked carbonization intermediate (Fig. 7d). The formed material underwent strong dehydration

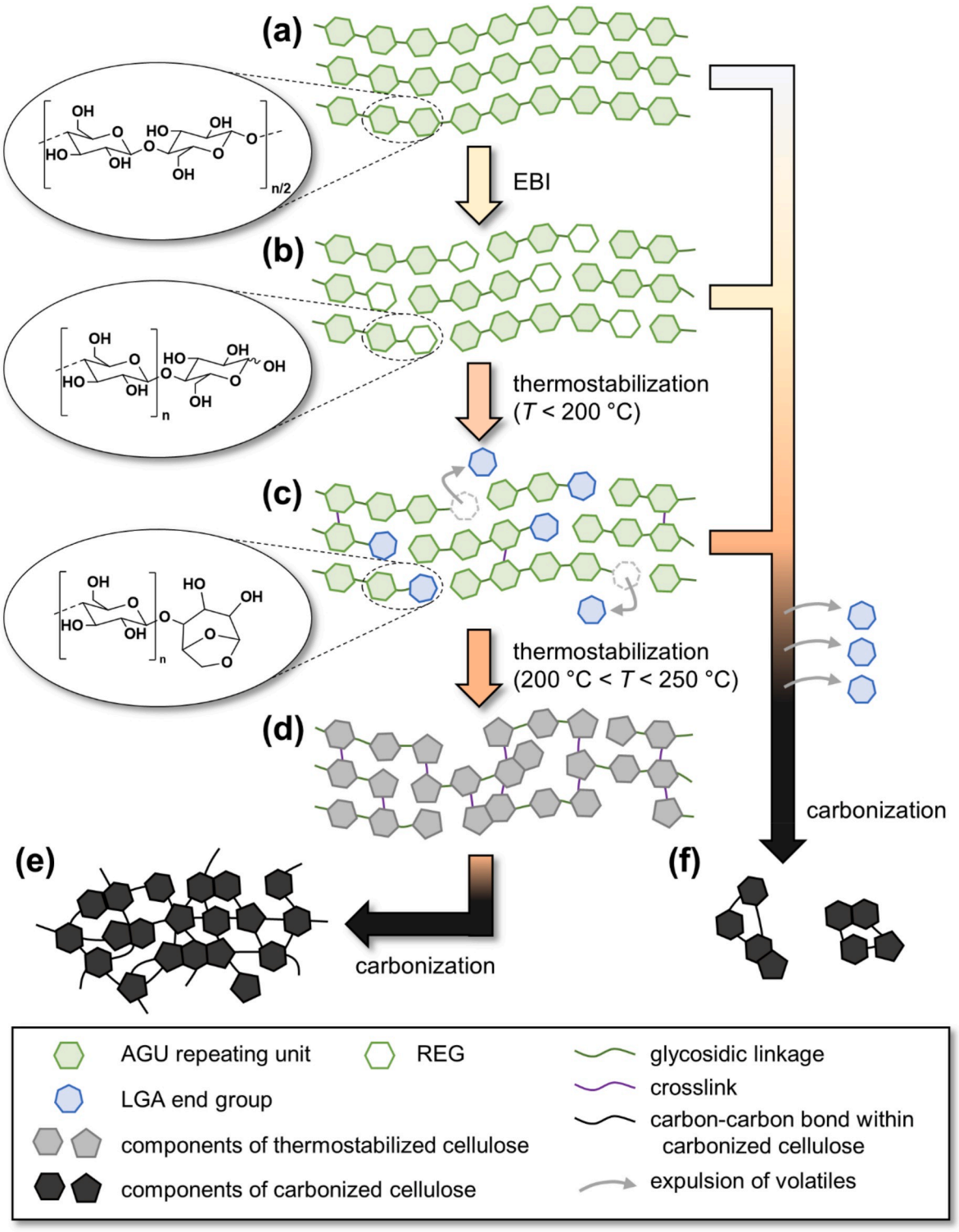

Fig. 7. Schematic illustration for the chemical transformations of cellulose observed in this work. (**a**) pristine cellulose, (**b**) irradiated cellulose, (**c**) thermostabilized cellulose ($T_{f,t}$ < 200 °C), (**d**) thermostabilized cellulose (200 °C < $T_{f,t}$ < 250 °C). Carbonization of sufficiently thermostabilized cellulose results in a high char yield (**e**), whereas in the other cases the occurrence of volatilization reactions leads to low char yields (**f**). (A colour version of this figure can be viewed online.)

reactions according to the FT-IR spectra and is presumably similar or related to the "thermostable condensed phase" reported by Pastorova *et al.* [69,70]. While we did not get further insights into the formed chemical structures or the mechanistic backgrounds to its formation, we believe that the reaction also initially occurs on the REGs liberated by the EBI treatment. The importance of REGs during cellulose pyrolysis and carbonization was recently highlighted in several reports [72–75]. As a result, the char yield of **C2E250S** (Fig. 7e) is higher than those of **C0E**, **C2E**, and **C2E200S** (Fig. 7f).

In addition, the significantly increased char yield in **C2E250S** (34.4 %) compared to **C1E250S** (24.6 %) can be also explained over the stronger fragmentation and resulting higher proportion of REGs caused by the harsher treatment, which can be transformed to a thermostable intermediate during heating in the temperature range of 200–250 °C.

3.3. EBI and thermostabilization of cellulose-lignin composite fibers

In addition to 100 % cellulose fibers, cellulose-lignin composite fibers were investigated in this study. We showed earlier how the carbon yield of cellulosic precursor filaments can be increased through the addition of lignin [18,31,36,57]. Also, 100 % cellulose precursor fibers require bleached dissolving grade pulp as substrate. The possibility to reduce the purity of the pulp and process also hemicellulose and lignin would reduce the raw material costs markedly. Thus, the effect of EBI on a cellulosic filament containing 30 wt% of lignin was investigated as next step, to examine the applicability of this pretreatment strategy for a broader scope of biobased precursors. Fig. 8a shows the ESR spectra of **CL0E**, **CL1E**, and **CL2E**. A weak signal was observed from the spectrum of pristine composite fibers (**CL0E**), presumably due to the presence of aromatic rings that can stabilize unpaired electrons temporarily present in the chemical structure of lignin. However, the ESR signal in the composite fibers became stronger with increasing electron beam dose. The shape of the newly introduced signal was different from that of the original signal observed in **CL0E**, but similar to those shown in the spectra of irradiated cellulose fibers (Fig. 2a). It has been reported that lignin is more resistant toward EBI compared to cellulose, which is presumably connected to its known radical scavenging properties [76]. Therefore, this ESR result confirmed that free radicals were generated from cellulose in the composite fiber, by the dissociation of glycosidic linkages as shown in Fig. 2c. Thus, we can expect a series of chemical reactions in the composite fibers during subsequent thermostabilization, which should be similar to the reactions in the cellulose fibers as described in the previous subsections. Fig. 8b shows TGA thermograms of **CL0E**, **CL1E250S**, and **CL2E250S**. Their relative residual mass at 1000 °C were 21.6, 33.2, and 42.5 %, respectively (see Table S3). Given the similar relative increases in residual mass as in the 100 % cellulose fibers, the EBI treatment predominantly seems to affect the cellulosic fraction, while no influence on the lignin fraction or synergistic effects were evident. The conclusions from this figure are identical to those from Fig. 5: i) the combination of EBI and the subsequent thermostabilization enhanced the char yield after carbonization, and ii) the higher electron beam dose resulted in the additional increase in the char yield. In addition, as readily observed in the case of thermostabilization of cellulose fibers, thermally induced repolymerization reactions at the temperature range of 200–250 °C are also crucial for irradiated cellulose-lignin composite fibers. Only **CL2E250S** showed a dramatic increase in the char yield (Fig. S3a), while the samples stabilized at lower temperatures had similar char yields as the non-treated precursors. Therefore, EBI was still effective even though cellulose, which is highly susceptible to electron beam, was blended with another polymer rich in aromatic units. This is attributed to the penetration efficiency of a high-energy electron beam, and the reactions during subsequent thermostabilization greatly contributed to the enhancement in the char yield of the composite fibers after carbonization.

3.4. Preparation of carbon fibers from cellulose and composite fibers

The insights gained through the thermostabilization studies were used to evaluate the practical applicability of EBI pretreatment in the preparation of carbon fibers and the effect on their mechanical properties. Fig. 9 shows optical micrographs and the change in diameter of cellulose and composite fibers by EBI, subsequent thermostabilization, and carbonization. The surface and cross-section of pristine and processed fibers were also examined with scanning electron microscopy (SEM, Fig. S4). The diameter of **C0E** (14.0 ± 0.4 μm) remained unchanged until the fiber was thermostabilized up to 200 °C. However, the first slight reduction in the diameter was observed after the fiber underwent thermal reactions at the temperature range of 200–250 °C, and subsequent carbonization led to a further decrease. As a result, the diameter of the resulting carbonized cellulose fiber (**C2ESC_2.0**) was 7.7 ± 0.9 μm. The SEM images did not show any macro-sized defects or voids on the surface and or across the cross-section of the fibers. We also observed an increase in the fibers' density after carbonization (1.47 → 1.63 g cm^{-3}), presumably because linear macromolecular cellulose chains were transformed into denser condensed structure through carbonization. The carbonization-induced densification of cellulose fibers is supported by the elemental analysis results (Fig. S2). The elemental fraction of carbon increased to 82 wt% after carbonization. The generation of D and G bands in the Raman spectrum of **C2ESC_2.0** verifies the presence of carbons in sp^2 configuration in the generated carbonaceous material (Fig. S5), which are superior to cellulose chains in terms of structural compactness. A similar change in the diameter (15.6 ± 0.7 → 8.2 ± 0.3 μm) and density (1.47 → 1.64 g cm^{-3}) was also observed for the cellulose-lignin fibers before and after carbonization.

Table 1 summarizes the results of tensile strength (σ), tensile modulus (E), and elongation at break (ε_b) for all carbonized fibers in this study. When the fibers were thermostabilized with rising temperature at a rapid heating ramp rate (2 °C/min), the mechanical properties of carbonized fibers derived from irradiated cellulose and composite fibers

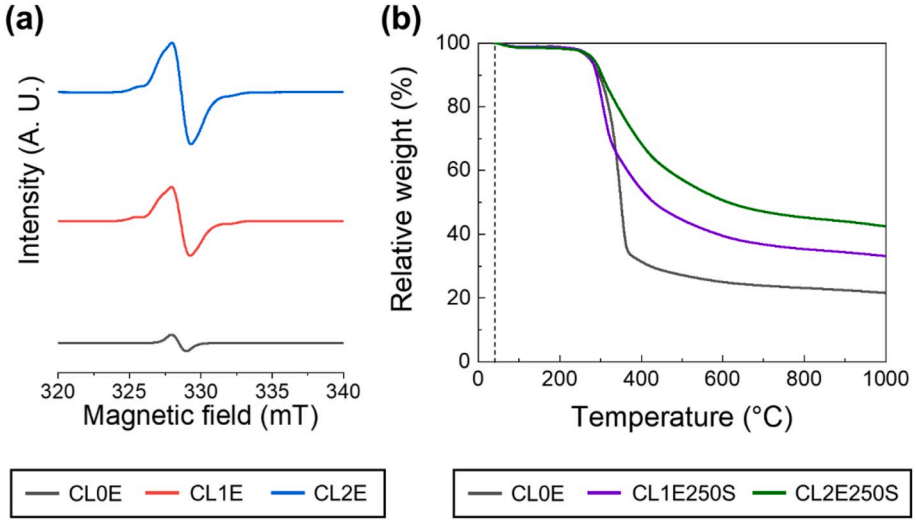

Fig. 8. (**a**) ESR spectra of pristine and irradiated cellulose-lignin composite fibers. (**b**) TGA thermograms (Ar) of pristine cellulose-lignin composite fibers and thermostabilized composite fibers after irradiation. Heating rate for the TGA analyses was 5 °C/min. The dashed vertical line indicates 40 °C, the initial temperature of the TGA analyses. (A colour version of this figure can be viewed online.)

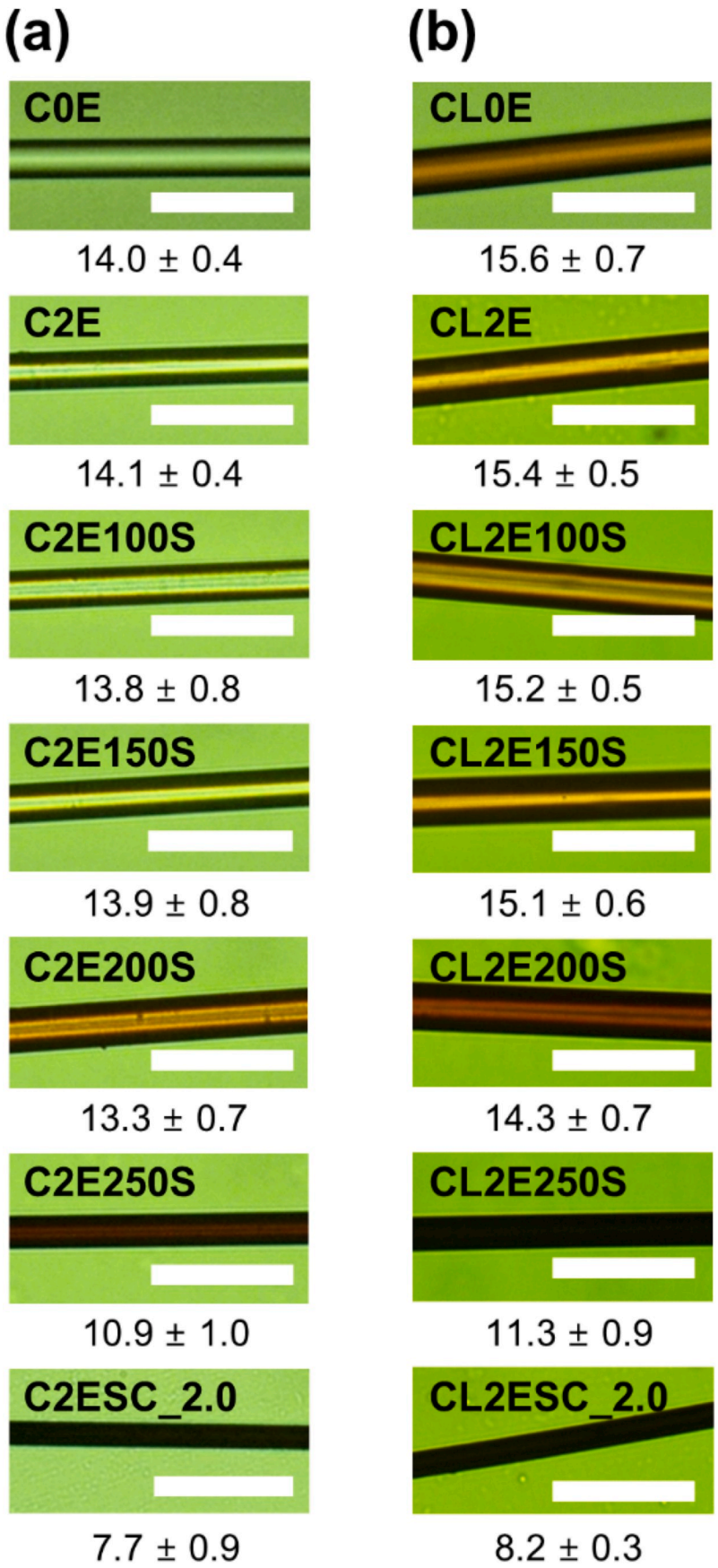

Fig. 9. Optical micrographs of (**a**) cellulose and (**b**) cellulose-lignin composite fibers before and after irradiation, thermostabilization with different $T_{f,t}$ and carbonization. (A colour version of this figure can be viewed online.)

Table 1
Mechanical properties of carbonized fibers.

Entry	Number of samples	σ (MPa)	E (GPa)	ε_b (%)
C2ESC_2.0	22	731 ± 87	38 ± 1.1	1.9 ± 0.2
C1ESC_2.0	23	639 ± 78	39 ± 2.4	1.6 ± 0.2
C0ESC_2.0	N/A			
C0ESC_1.0	21	594 ± 89	39 ± 0.9	1.5 ± 0.2
C0ESC_0.5	17	713 ± 88	41 ± 2.1	1.7 ± 0.3
C0ESC_0.2	14	736 ± 88	40 ± 1.5	1.8 ± 0.2
CL2ESC_2.0	17	651 ± 133	40 ± 1.6	1.7 ± 0.4
CL1ESC_2.0	15	623 ± 137	41 ± 0.8	1.7 ± 0.3
CL0ESC_2.0	N/A			

were measurable, whereas **C0ESC_2.0** was too brittle for single fiber testing. This result indicates that the pristine cellulose fibers cannot be transformed into mechanically durable carbon structures after carbonization with such a rapid thermostabilization process. Conversely, irradiated fibers that were thermostabilized even at a heating rate of 2 °C/min resulted in thermally more stable and mechanically stronger fibers after carbonization. Based on TGA (Fig. 5) and FT-IR (Fig. 6) data, we believe that the introduction of C═O and C═C bonds during thermostabilization and the increased char yield after carbonization are closely related to the structural integrity of the resulting carbonaceous materials derived from irradiated cellulose. In addition, the tensile strength and modulus of **C2ESC_2.0** were higher than those of **C1ESC_2.0**, and those difference were statistically significant. Therefore, the increase in the char yield is connected to the improved mechanical properties of the resulting carbonized fibers. EBI played a significant role in the fabrication of carbonized fibers from cellulose fibers with quantifiable mechanical properties.

Nevertheless, non-irradiated cellulose fibers could be converted to carbonized fibers with measurable mechanical properties, provided that the heating rate during thermostabilization was lower than 2 °C/min. For example, single fiber tests were possible for **C0ESC_1.0**, **C0ESC_0.5**, and **C0ESC_0.2**, and the mechanical properties of **C0ESC_0.2** were similar to those of **C2ESC_2.0**. However, it should be noted here that tensile strengths of **C0ESC_0.5** and **C0ESC_0.2** are equal in the statistical point of view. Therefore, compared to the time required for the thermostabilization with the heating rate of 0.5 °C/min, we could considerably reduce the process duration by a factor of four (400 min → 100 min) when the environmental temperature was increased from 50 to 250 °C with the rate of 2 °C/min, reaffirming the acceleration effect of EBI for the thermostabilization of cellulose fibers. The accelerated thermostabilization was also observed in the carbonization of cellulose-lignin composite fibers; Table 1 shows that **CL0ESC_2.0** was as brittle as **C0ESC_2.0**, while the mechanical properties of **CL1ESC_2.0** and **CL2ESC_2.0** were measurable even with a rapid heating rate (2 °C/min). Unlike in the case of carbonized cellulose fibers, tensile strengths and elongation at breaks of **CL1ESC_2.0** and **CL2ESC_2.0** were statistically similar except for their tensile moduli.

Thermal conductivity is one of significant properties related to crystallinity and mechanical strength/modulus of carbon fibers. The DC self-heating method was utilized to evaluate the thermal conductivity of carbon fibers, and we confirmed the reliability of this method from the similarity between the measured thermal conductivity of T700S (9.80 W/m•K) and the value noted in the technical data sheet provided by its manufacturer (9.6 W/m•K). The thermal conductivity of **C2ESC_2.0** (5.89 W/m•K) was lower than that of PAN-based T700S, and this significant reduction in conductivity is attributable to their low crystallinity and mechanical properties of biomass-derived carbon fibers. This value can be considered low among thermal conductivities of other cellulose-based carbon fibers found in the literature (5–15 W/m•K) [77]. Furthermore, a slightly lower conductivity was observed in **CL2ESC_2.0** (4.23 W/m•K), which may be ascribed to its intrinsic low thermal conductivity of carbonized lignin [78]. Therefore, once the manufacturing process is optimized to enhance their mechanical properties, we believe that our cellulose and lignin-based carbon fibers could also be used in applications requiring thermally insulative carbon fibers with modest mechanical strength.

4. Conclusion and outlook

In this study the effect of EBI treatments for cellulosic CF precursors was investigated as an advantageous dry chemical pretreatment strategy. Emphasis was laid on a thorough chemical analysis of the prepared materials to obtain a better understanding of the operative mechanisms. It was found that EBI treatment predominantly results in the fragmentation of cellulose chains down to oligomers under liberation of REGs. Additionally, oxidation reactions were evident, however, only to a small extent.

By performing systematic thermostabilization experiments in combination with TGA and DSC thermal analyses, it was found that EBI treatment alone is insufficient to significantly increase char yields compared to the pristine fibers. Only after conducting thermostabilization by heating between 200 °C and 250 °C reactions occur that transform the cellulosic precursors to a thermally stable intermediate. Given the strong proportion of REGs in the EBI treated fibers and the accumulating literature on the general importance of reducing ends during cellulose pyrolysis and carbonization [72–75], we postulate that the reactions leading to the thermally stable phase are predominantly occurring on this more reactive end moiety. The performed analytical characterization of the sufficiently thermostabilized precursors ($T_{f,t}$ = 250 °C) hinted towards significant chemical transformations under dehydration, polycondensation and destruction of the polysaccharidic nature of the material [69,70]. However, we were unable to get further insights in the operative mechanism or the formed structures in this study. Intriguingly, the strong fragmentation caused by the EBI treatment resulted in higher char yields as it enabled subsequent dehydrating "crosslinking" reactions during thermostabilization. This contrasts with reports where an increase of the molecular weight by direct crosslinking of the AGU moieties is connected with increased char yields [55].

EBI-assisted thermostabilization of cellulose fibers can improve the economic feasibility of (ligno-) cellulose-derived carbon fiber. It allowed to significantly increase the char yield for pure cellulose fibers from 12.1 % to 34.4 % and for cellulose lignin blends from 21.6 % to 38.9 %. Furthermore, the time required for thermostabilization could be reduced by a factor of 4, and we are optimistic that this can be further optimized in future follow-up investigations.

CRediT authorship contribution statement

Minjeong Jang: Formal analysis, Investigation, Writing – original draft. **Lukas Fliri:** Formal analysis, Investigation, Writing – original draft. **Mikaela Trogen:** Investigation. **Dongcheon Choi:** Investigation. **Jeong-Heum Han:** Investigation. **Jungwon Kim:** Supervision, Writing – review & editing. **Sung-Kon Kim:** Formal analysis, Supervision. **Sungho Lee:** Conceptualization, Methodology, Writing – review & editing. **Sung-Soo Kim:** Conceptualization, Methodology, Validation, Supervision, Writing – original draft, Project administration. **Michael Hummel:** Conceptualization, Methodology, Validation, Supervision, Writing – original draft, Project administration.

Declaration of competing interest

The authors declare that they have no known competing financial interests or personal relationships that could have appeared to influence the work reported in this paper.

Acknowledgements

This research was supported by the National Research Council of Science & Technology (NST) grants by the Korea government (MSIT)

[grant number: CAP22091-000 and CRC23011-000], and National R&D Program through the National Research Foundation of Korea (NRF) grant funded by the Korea government (MSIT) [grant number: 2021M3H4A1A03041296]. LF and MH gratefully acknowledge funding from the Academy of Finland (projects: 348354 and 353841) and financial support by the Foundation of Walter Ahlström. Authors are grateful to Youn-Mook Lim and Huisu Kim of Korea Atomic Energy Research Institute for his valuable advice and suggestion for this work.

Appendix A. Supplementary data

Supplementary data to this article can be found online at https://doi.org/10.1016/j.carbon.2023.118759.

References

[1] P. Bajaj, A. Roopanwal, Thermal stabilization of acrylic precursors for the production of carbon fibers: an overview, J. Macromol. Sci. Polym. Rev. 37 (1997) 97.
[2] S. Nunna, M. Naebe, N. Hameed, B.L. Fox, C. Creighton, Evolution of radial heterogeneity in polyacrylonitrile fibres during thermal stabilization: an overview, Polym. Degrad. Stabil. 136 (2017) 20.
[3] M. Smith, New developments in carbon fiber, Reinforc Plast 62 (2018) 266.
[4] C. Soutis, Carbon fiber reinforced plastics in aircraft construction, Mater. Sci. Eng. 412 (2005) 171.
[5] A. Lewandowska, C. Soutis, L. Savage, S.J. Eichhorn, Carbon fibres with ordered graphitic-like aggregate structures from a regenerated cellulose fibre precursor, Compos. Sci. Technol. 116 (2015) 50.
[6] E. Frank, L.M. Steudle, D. Ingildeev, J.M. Spörl, M.R. Buchmeiser, Carbon fibers: precursor systems, processing, structure, and properties, Angew. Chem. Int. Ed. 53 (2014) 5262.
[7] A. Zaitsev, S. Moisan, F. Poncin-Epaillard, Cellulose carbon fiber: plasma synthesis and characterization, Cellulose 28 (2021) 1973.
[8] J. Liu, X. Chen, D. Liang, Q. Xie, Development of pitch-based carbon fibers: a review, Energy Sources, Part A Recovery, Util. Environ. Eff. 1 (2020).
[9] V. Prada, M. Granda, J. Bermejo, R. Menéndez, Preparation of novel pitches by tar air-blowing, Carbon 37 (1999) 97.
[10] A.H. Wazir, L. Kakakhel, Preparation and characterization of pitch-based carbon fibers, N. Carbon Mater. 24 (2009) 83.
[11] G. Bolan, G.-Z. Liu, T. Hochgeschurtz, M. Thies, Producing a carbon fiber precursor by supercritical fluid extraction, Fluid Phase Equil. 82 (1993) 303.
[12] P.-P. Li, J.-M. Xiong, M.-L. Ge, J.-C. Sun, W. Zhang, Y.-Y. Song, Preparation of pitch-based general purpose carbon fibers from catalytic slurry oil, Fuel Process. Technol. 140 (2015) 231.
[13] C. Ge, H. Yang, J. Miyawaki, I. Mochida, S.-H. Yoon, W. Qiao, D. Long, L. Ling, Synthesis and characterization of high-softening-point methylene-bridged pitches by visible light irradiation assisted free-radical bromination, Carbon 95 (2015) 780.
[14] E. Mora, R. Santamaría, C. Blanco, M. Granda, R. Menendez, Mesophase development in petroleum and coal-tar pitches and their blends, J. Anal. Appl. Pyrol. 68 (2003) 409.
[15] L.M. Heidbreder, I. Bablok, S. Drews, C. Menzel, Tackling the plastic problem: a review on perceptions, behaviors, and interventions, Sci. Total Environ. 668 (2019) 1077.
[16] M. MacLeod, H.P.H. Arp, M.B. Tekman, A. Jahnke, The global threat from plastic pollution, Science 373 (2021) 61.
[17] Review on the precursor preparation and carbon fiber manufacturing, in: Z. Lu (Ed.), Journal of Physics: Conference Series, IOP Publishing, 2021.
[18] N.-D. Le, M. Trogen, Y. Ma, R.J. Varley, M. Hummel, N. Byrne, Cellulose-lignin composite fibers as precursors for carbon fibers: Part 2–The impact of precursor properties on carbon fibers, Carbohydr. Polym. 250 (2020) 116918.
[19] A. Milbrandt, S. Booth, Carbon Fiber from Biomass, National Renewable Energy Lab.(NREL), Golden, CO (United States), 2016.
[20] X. Zhang, Y. Lu, H. Xiao, H. Peterlik, Effect of hot stretching graphitization on the structure and mechanical properties of rayon-based carbon fibers, J. Mater. Sci. 49 (2014) 673.
[21] L. Kobets, I. Deev, Carbon fibres: structure and mechanical properties, Compos. Sci. Technol. 57 (1998) 1571.
[22] A. Broido, M.A. Nelson, Char yield on pyrolysis of cellulose, Combust. Flame 24 (1975) 263.
[23] P.H. Brunner, P.V. Roberts, The significance of heating rate on char yield and char properties in the pyrolysis of cellulose, Carbon 18 (1980) 217.
[24] D.F. Arseneau, Competitive reactions in the thermal decomposition of cellulose, Can. J. Chem. 49 (1971) 632.
[25] A.G. Bradbury, Y. Sakai, F. Shafizadeh, A kinetic model for pyrolysis of cellulose, J. Appl. Polym. Sci. 23 (1979) 3271.
[26] M.J. Antal, A review of the literature Part 1-carbohydrate pyrolysis, in: K.W. Boer, V.A. Duffie (Eds.), Advances in Solar Energy, vol. 2, American Solar Energy Society, New York, NY, 1985, p. 175.
[27] A.E. Lipska, W.J. Parker, Kinetics of the pyrolysis of cellulose in the temperature range 250–300° C, J. Appl. Polym. Sci. 10 (1966) 1439.
[28] G.-J. Kwon, D.-Y. Kim, K.-Y. Kang, Effects of low-temperature pretreatment on carbonization of cellulose for the production of biocarbons, J. Kor. Phys. Soc. 60 (2012) 1814.
[29] A. Bridgwater, S. Czernik, J. Diebold, D. Meier, A. Oasmaa, C. Peacocke, J. Piskorz, D. Radlein, Fast Pyrolysis of Biomass: a Handbook, 1999.
[30] C. Di Blasi, C. Branca, A. Galgano, Flame retarding of wood by impregnation with boric acid–pyrolysis products and char oxidation rates, Polym. Degrad. Stabil. 92 (2007) 752.
[31] N.-D. Le, M. Trogen, R.J. Varley, M. Hummel, N. Byrne, Effect of boric acid on the stabilisation of cellulose-lignin filaments as precursors for carbon fibres, Cellulose 28 (2021) 729.
[32] D. Choi, H.-S. Kil, S. Lee, Fabrication of low-cost carbon fibers using economical precursors and advanced processing technologies, Carbon 142 (2019) 610.
[33] N.-D. Le, M. Trogen, R.J. Varley, M. Hummel, N. Byrne, Chemically accelerated stabilization of a cellulose–lignin precursor as a route to high yield carbon fiber production, Biomacromolecules 23 (2022) 839.
[34] J.M. Spörl, R. Beyer, F. Abels, T. Cwik, A. Müller, F. Hermanutz, M.R. Buchmeiser, Cellulose-derived carbon fibers with improved carbon yield and mechanical properties, Macromol. Mater. Eng. 302 (2017) 1700195.
[35] Effect of flame retardants on pyrolysis and combustion of α-cellulose, in: W. K. Tang, W.K. Neill (Eds.), Journal of Polymer Science Part C: Polymer Symposia, Wiley Online Library, 1964.
[36] R. Gong, Z. Ma, X. Wang, Y. Han, Y. Guo, G. Sun, Y. Li, J. Zhou, Sulfonic-acid-functionalized carbon fiber from waste newspaper as a recyclable carbon based solid acid catalyst for the hydrolysis of cellulose, RSC Adv. 9 (2019) 28902.
[37] A.G. Dumanlı, A.H. Windle, Carbon fibres from cellulosic precursors: a review, J. Mater. Sci. 47 (2012) 4236.
[38] B.K. Kandola, A. Horrocks, D. Price, G. Coleman, Flame-retardant treatments of cellulose and their influence on the mechanism of cellulose pyrolysis, J. Macromol. Sci. Polym. Rev. 36 (1996) 721.
[39] Y. Long, Y. Yu, Y.W. Chua, H. Wu, Acid-catalysed cellulose pyrolysis at low temperatures, Fuel 193 (2017) 460.
[40] D.-Y. Kim, Y. Nishiyama, M. Wada, S. Kuga, High-yield carbonization of cellulose by sulfuric acid impregnation, Cellulose 8 (2001) 29.
[41] G. Dobele, G. Rossinskaja, G. Telysheva, D. Meier, O. Faix, Cellulose dehydration and depolymerization reactions during pyrolysis in the presence of phosphoric acid, J. Anal. Appl. Pyrol. 49 (1999) 307.
[42] M.P. Vocht, A. Ota, E. Frank, F. Hermanutz, M.R. Buchmeiser, Preparation of cellulose-derived carbon fibers using a new reduced-pressure stabilization method, Ind. Eng. Chem. Res. 61 (2022) 5191.
[43] M. Jang, D. Choi, Y. Kim, H.-S. Kil, S.-K. Kim, S.M. Jo, S. Lee, S.-S. Kim, Role of sulfuric acid in thermostabilization and carbonization of lyocell fibers, Cellulose (2023) 1.
[44] K. Kolářová, V. Vosmanská, S. Rimpelová, V. Švorčík, Effect of plasma treatment on cellulose fiber, Cellulose 20 (2013) 953.
[45] S.-W. Lee, H.-Y. Lee, S.-Y. Jang, S. Jo, H.-S. Lee, W.-H. Choe, S. Lee, Efficient preparation of carbon fibers using plasma assisted stabilization, Carbon 55 (2013) 361.
[46] S.-Y. Kim, S. Lee, S. Park, S.M. Jo, H.-S. Lee, H.-I. Joh, Continuous and rapid stabilization of polyacrylonitrile fiber bundles assisted by atmospheric pressure plasma for fabricating large-tow carbon fibers, Carbon 94 (2015) 412.
[47] H.-H. Chien, K.-J. Ma, C.-H. Kuo, S.-W. Huang, Effects of plasma power and reaction gases on the surface properties of ePTFE materials during a plasma modification process, Surf. Coating. Technol. 228 (2013) S477.
[48] J. Moosburger-Will, E. Lachner, M. Löffler, C. Kunzmann, M. Greisel, K. Ruhland, S. Horn, Adhesion of carbon fibers to amine hardened epoxy resin: influence of ammonia plasma functionalization of carbon fibers, Appl. Surf. Sci. 453 (2018) 141.
[49] D. Cho, H.S. Lee, S.O. Han, L.T. Drzal, Effects of E-beam treatment on the interfacial and mechanical properties of henequen/polypropylene composites, Adv. Compos. Mater. 16 (2007) 315.
[50] H. Stupińska, E. Iller, Z. Zimek, D. Wawro, D. Ciechańska, E. Kopania, J. Palenik, S. Milczarek, W. Stęplewski, G. Krzyżanowska, An Environment-Friendly Method to Prepare Microcrystalline Cellulose, Fibres & Textiles in Eastern Europe, 2007, p. 167.
[51] S. Park, S.H. Yoo, H.R. Kang, S.M. Jo, H.-I. Joh, S. Lee, Comprehensive stabilization mechanism of electron-beam irradiated polyacrylonitrile fibers to shorten the conventional thermal treatment, Sci. Rep. 6 (2016) 27330.
[52] H.K. Shin, M. Park, H.-Y. Kim, S.-J. Park, An overview of new oxidation methods for polyacrylonitrile-based carbon fibers, Carbon Lett. 16 (2015) 11.
[53] S.H. Yoo, S. Park, Y. Park, D. Lee, H.-I. Joh, I. Shin, S. Lee, Facile method to fabricate carbon fibers from textile-grade polyacrylonitrile fibers based on electron-beam irradiation and its effect on the subsequent thermal stabilization process, Carbon 118 (2017) 106.
[54] U. Henniges, M. Hasani, A. Potthast, G. Westman, T. Rosenau, Electron beam irradiation of cellulosic materials—opportunities and limitations, Materials 6 (2013) 1584.
[55] M.I. Kim, M.-S. Park, Y.-S. Lee, Cellulose-based carbon fibers prepared using electron-beam stabilization, Carbon Lett. 18 (2016) 56.
[56] L. Fliri, K. Heise, T. Koso, A.R. Todorov, D.R. Del Cerro, S. Hietala, J. Fiskari, I. Kilpeläinen, M. Hummel, A.W. King, Solution-state nuclear magnetic resonance spectroscopy of crystalline cellulosic materials using a direct dissolution ionic liquid electrolyte, Nat. Protoc. (2023) 1.
[57] M. Trogen, N.-D. Le, D. Sawada, C. Guizani, T.V. Lourençon, L. Pitkänen, H. Sixta, R. Shah, H. O'Neill, M. Balakshin, Cellulose-lignin composite fibres as precursors

for carbon fibres. Part 1–Manufacturing and properties of precursor fibres, Carbohydr. Polym. 252 (2021) 117133.
[58] T. Koso, D. Rico del Cerro, S. Heikkinen, T. Nypelö, J. Buffiere, J.E. Perea-Buceta, A. Potthast, T. Rosenau, H. Heikkinen, H. Maaheimo, 2D Assignment and quantitative analysis of cellulose and oxidized celluloses using solution-state NMR spectroscopy, Cellulose 27 (2020) 7929.
[59] A.W. King, V. Mäkelä, S.A. Kedzior, T. Laaksonen, G.J. Partl, S. Heikkinen, H. Koskela, H.A. Heikkinen, A.J. Holding, E.D. Cranston, Liquid-state NMR analysis of nanocelluloses, Biomacromolecules 19 (2018) 2708.
[60] L. Fliri, C. Guizani, I.Y. Miranda-Valdez, L. Pitkänen, M. Hummel, Reinvestigating the concurring reactions in early-stage cellulose pyrolysis by solution state NMR spectroscopy, J. Anal. Appl. Pyrol. 175 (2023) 106153.
[61] J. Moon, K. Weaver, B. Feng, H.G. Chae, S. Kumar, J.B. Baek, G.P. Peterson, Note: thermal conductivity measurement of individual poly(ether ketone)/carbon nanotube fibers using a steady-state dc thermal bridge method, Rev. Sci. Instrum. 83 (2012) 016103.
[62] A. Alberti, S. Bertini, G. Gastaldi, N. Iannaccone, D. Macciantelli, G. Torri, E. Vismara, Electron beam irradiated textile cellulose fibres.: ESR studies and derivatisation with glycidyl methacrylate (GMA), Eur. Polym. J. 41 (2005) 1787.
[63] A. Khan, J. Labrie, J. McKeown, Effect of electron-beam irradiation pretreatment on the enzymatic hydrolysis of softwood, Biotechnol. Bioeng. 28 (1986).
[64] B.-M. Lee, J.-Y. Lee, D.-Y. Kim, S.-K. Hong, P.-H. Kang, J.-P. Jeun, Environmentally-friendly Pretreatment of Rice Straw by an Electron Beam Irradiation, 2014.
[65] J.S. Bak, Electron beam irradiation enhances the digestibility and fermentation yield of water-soaked lignocellulosic biomass, Biotechnology Rep. 4 (2014) 30.
[66] J. Simon, L. Fliri, J. Sapkota, M. Ristolainen, S.A. Miller, M. Hummel, T. Rosenau, A. Potthast, Reductive amination of dialdehyde cellulose: access to renewable thermoplastics, Biomacromolecules 24 (2022) 166.
[67] T. Hosoya, M. Bacher, A. Potthast, T. Elder, T. Rosenau, Insights into degradation pathways of oxidized anhydroglucose units in cellulose by β-alkoxy-elimination: a combined theoretical and experimental approach, Cellulose 25 (2018) 3797.
[68] X. Zhang, W. Yang, C. Dong, Levoglucosan formation mechanisms during cellulose pyrolysis, J. Anal. Appl. Pyrol. 104 (2013) 19.
[69] I. Pastorova, R.E. Botto, P.W. Arisz, J.J. Boon, Cellulose char structure: a combined analytical Py-GC-MS, FTIR, and NMR study, Carbohydr. Res. 262 (1994) 27.
[70] I. Pastorova, P.W. Arisz, J.J. Boon, Preservation of d-glucose-oligosaccharides in cellulose chars, Carbohydr. Res. 248 (1993) 151.
[71] H. Kawamoto, Review of reactions and molecular mechanisms in cellulose pyrolysis, Curr. Org. Chem. 20 (2016) 2444.
[72] E. Leng, M. Costa, Y. Peng, Y. Zhang, X. Gong, A. Zheng, Y. Huang, M. Xu, Role of different chain end types in pyrolysis of glucose-based anhydro-sugars and oligosaccharides, Fuel 234 (2018) 738.
[73] Q. Lu, B. Hu, Z-x Zhang, Y-t Wu, M-s Cui, D-j Liu, C-q Dong, Y-p Yang, Mechanism of cellulose fast pyrolysis: the role of characteristic chain ends and dehydrated units, Combust. Flame 198 (2018) 267.
[74] S. Matsuoka, H. Kawamoto, S. Saka, Thermal glycosylation and degradation reactions occurring at the reducing ends of cellulose during low-temperature pyrolysis, Carbohydr. Res. 346 (2011) 272.
[75] S. Matsuoka, H. Kawamoto, S. Saka, What is active cellulose in pyrolysis? An approach based on reactivity of cellulose reducing end, J. Anal. Appl. Pyrol. 106 (2014) 138.
[76] O. Sarosi, I. Sulaeva, E. Fitz, I. Sumerskii, M. Bacher, A. Potthast, Lignin resists high-intensity electron beam irradiation, Biomacromolecules 22 (2021) 4365.
[77] F. Panerai, J.C. Ferguson, J. Lachaud, A. Martin, M.J. Gasch, N.N. Mansour, Micro-tomography based analysis of thermal conductivity, diffusivity and oxidation behavior of rigid and flexible fibrous insulators, Int. J. Heat Mass Tran. 108 (2017) 801.
[78] J. Liu, W. Qu, Y. Xie, B. Zhu, T. Wang, X. Bai, X. Wang, Thermalconductivity and annealing effect on structure of lignin-based microscale carbon fibers, Carbon 121 (2017) 35.